3-Amino-benzo[*d*]isoxazoles as Novel Multitargeted Inhibitors of Receptor Tyrosine Kinases

Zhiqin Ji,*,† Asma A. Ahmed,‡ Daniel H. Albert,† Jennifer J. Bouska,† Peter F. Bousquet,‡ George, A. Cunha,‡ Gilbert Diaz,† Keith B. Glaser,† Jun Guo,† Christopher M. Harris,‡ Junling Li,† Patrick A. Marcotte,† Maria D. Moskey,‡ Tetsuro Oie,† Lori Pease,† Nirupama B. Soni,† Kent D. Stewart,† Steven K. Davidsen,† and Michael R. Michaelides†

Global Pharmaceutical Research and Development, Abbott Laboratories, 100 Abbott Park Road, Abbott Park, Illinois 60064-6100, and Abbott Bioresearch Center, 100 Research Drive, Worcester, Massachusetts 01605-5314

Received September 4, 2007

A series of benzoisoxazoles and benzoisothiazoles have been synthesized and evaluated as inhibitors of receptor tyrosine kinases (RTKs). Structure–activity relationship studies led to the identification of 3-amino benzo[*d*]isoxazoles, incorporating a *N*,*N*′-diphenyl urea moiety at the 4-position that potently inhibited both the vascular endothelial growth factor receptor (VEGFR) and platelet-derived growth factor receptor families of RTKs. Within this series, orally bioavailable compounds possessing promising pharmacokinetic profiles were identified, and a number of compounds demonstrated in vivo efficacy in models of VEGF-stimulated vascular permeability and tumor growth. In particular, compound **50** exhibited an ED_{50} of 2.0 mg/kg in the VEGF-stimulated uterine edema model and 81% inhibition in the human fibrosarcoma (HT1080) tumor growth model when given orally at a dose of 10 mg/kg/day.

Introduction

Receptor tyrosine kinases (RTKs[a]), a subclass of cell surface growth factor receptors, mediate cellular response to environmental signals and facilitate a broad range of cellular processes including proliferation, migration, and survival.[1,2] RTK signaling pathways are normally highly regulated. However, aberrant activation of RTKs, in particular, vascular endothelial growth factor receptor (VEGFR) and platelet-derived growth factor receptor (PDGFR), has been linked to the development and progression of various human cancers.[3–5] The VEGFR family, comprised of FLT1 (VEGFR1), KDR (VEGFR2), and FLT4 (VEGFR3), plays a pivotal role in angiogenesis and contributes to tumor progression through its ability to mediate tumor angiogenesis and lymphangiogenesis, and to enhance vascular permeability.[6–10] The PDGFR family, consisting of PDGFR-α, PDGFR-β, colony stimulating factor 1 receptor (CSF1R), KIT, and FLT3, promotes tumor cell growth and metastasis through modification of the tumor microenvironment.[11,12] Additionally, mutations of FLT3 and KIT are directly associated with proliferation of acute myeloid leukemia (AML) blast cells and gastrointestinal stromal tumor (GIST) cells, respectively.[13–18]

Inhibition of RTK signaling pathways has become an important area of new cancer drug discovery.[19–21] The approval of bevacizumab,[22] an anti-VEGF antibody, and the antitumor efficacy exhibited by small molecule inhibitors such as (*Z*)-3-((3,5-dimethyl-1*H*-pyrrol-2-yl)methylene)indolin-2-one (SU5416),[23] *N*-(4-chlorophenyl)-4-(pyridin-4-ylmethyl)phthalazin-1-amine (PTK787, vatalanib),[24,25] and 3-(4-bromo-2,6-difluorobenzyloxy)-5-(3-(4-(pyrrolidin-1-yl)butyl)ureido)isothiazole-4-carboxamide (CP-547632)[26] have established VEGFR as an important target for therapeutic intervention. Although VEGFR and PDGFR are compelling cancer targets individually, tumors are capable of secreting multiple angiogenic factors and they depend on these factors at different stages of progression.[27–29] For example, VEGFs cause a large increase in blood vessel formation, yet these vessels are immature and leaky. The formation of thicker, more stable vessels requires encapsulation by pericytes that are driven by PDGFR-β signaling. The multifactorial mechanisms by which cancer cells proliferate demand the development of multitargeted agents to interfere with multiple pathways. Simultaneous blockade of all the VEGF and PDGF receptors is expected to provide a synergistic effect by impacting multiple stages of tumor formation and, thus, may offer greater potential for treating a broader range of human cancers. The recent approval of the multitargeted agents **1** (sunitinib)[30] and **2** (sorafenib)[31] demonstrates that clinical benefit with manageable side effects is possible with broad-acting kinase inhibitors (Figure 1). As part of a research program at Abbott aiming at the identification of novel multitargeted RTK inhibitors, we have explored several chemotypes such as thienopyrimidines,[32] isothiazolopyrimidines,[33] thienopyridines,[34] and indazoles[35] as potent inhibitors of multitargeted RTKs. Extensive SAR studies in the aminoindazole series led to the discovery of **3** (ABT-869),[35,36] which is currently in phase **II** clinical trials.

A model of **3** docked into the active site of KDR in its inactive conformation shows that the 3-amino group along with its adjacent ring nitrogen serves as an anchor binding to the hinge region of KDR, while the diaryl urea moiety extends into the hydrophobic back pocket of the kinase domain (Figure 2). According to this model, the endocyclic indazole N1-H of **3** does not form additional hydrogen bonds with the kinase, and SAR studies confirm that methylation of the N1-H only results in a slight loss in KDR potency.[35] Based on these observations, we rationalize that the N1-H of endocyclic indazole can be replaced by oxygen or sulfur, leading to the novel chemotypes aminobenzoisoxazole (**4**) and aminobenzoisothiazole (**5**; Figure

* To whom correspondence should be addressed. Tel.: (847) 938-9442. Fax: (847) 935-5165. E-mail: zhiqin.ji@abbott.com.

† Abbott Laboratories.

‡ Abbott Bioresearch Center.

[a] Abbreviations: RTK, receptor tyrosine kinase; VEGFR, vascular endothelial growth factor receptor; PDGFR, platelet-derived growth factor receptor; FLT, Fms-like tyrosine kinase; KDR, kinase insert domain-containing receptor tyrosine kinase; CSF1R, colony stimulating factor 1 receptor; AML, acute myeloid leukemia; GIST, gastrointestinal stromal tumor; ATP, adenosine 5′-triphosphate; FGFR, fibroblast growth factor receptor; UE, uterine edema.

10.1021/jm701096v CCC: $40.75
Published on Web 02/09/2008

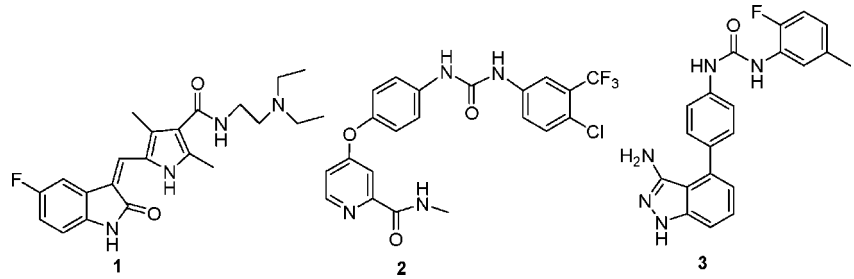

Figure 1. Advanced multitargeted RTK inhibitors.

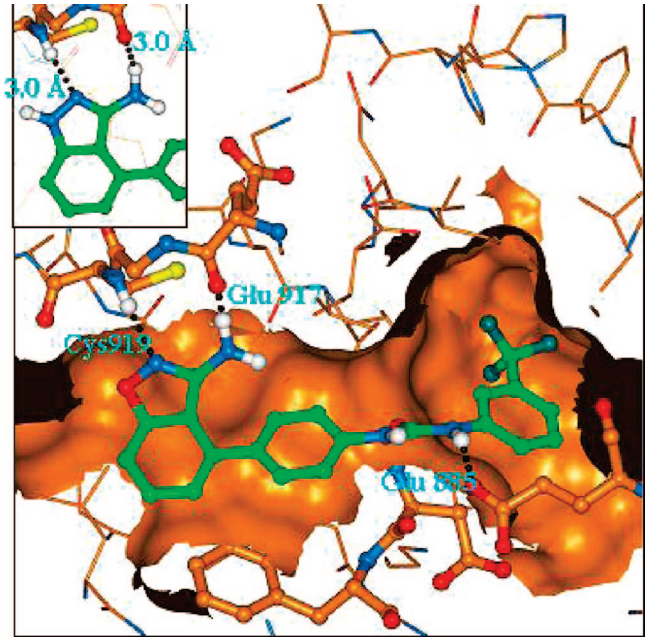

Figure 2. Molecular models of inhibitors bound to the inactive conformation of KDR (based on cKit crystal structure). The inset shows the previously described interaction of compound **3** with two hydrogen bonds to the hinge region. The larger picture shows model of aminobenzisoxazole **14** bound to KDR with two analogous hinge hydrogen bonds to Glu 917 and Cys 919. The urea of **14** donates a hydrogen bond to Glu 885.

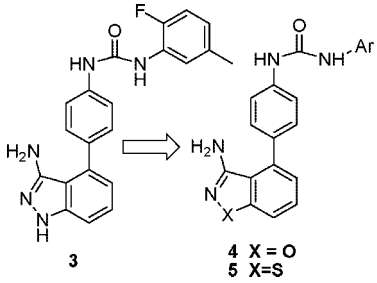

Figure 3. Inhibitor design.

3). We wish to report the effects of these replacements on structure–activity relationships, pharmacokinetics, and in vivo efficacy.

Chemistry

The general synthetic route for the preparation of 3-aminobenzoisoxazole derivatives is shown in Scheme 1. Treatment of commercially available **6** with acetohydroxamic acid and potassium *t*-butoxide provided the core 3-aminobenzisoxazole **7**, which underwent Suzuki coupling with 4-(4,4,5,5-tetramethyl-[1,3,2]dioxaborolan-2-yl)-phenylamine to afford aniline **8**. Compound **8** served as a key intermediate for the preparation of a number of target molecules. For example, urea **9** was prepared by the treatment of **8** with NaOCN in acetic acid solution; **10** and **11** were synthesized by the reaction of **8** with carboxylic acid chlorides. Treatment of **8** with the requisite isocyanates gave rise to the corresponding urea analogs **13** and **14**. To confirm the regioselectivity of the reaction of **8** with isocyanates, we also prepared **13** and **14** via Suzuki coupling of **7** with urea boronates **12a**,**b**, which were readily prepared via the treatment of 4-(4,4,5,5-tetramethyl-[1,3,2]dioxaborolan-2-yl)-phenylamine with the appropriate isocyanates. The products obtained from both methods were identical. Consequently, urea analogs **23**–**45** were prepared by treatment of **8** with the corresponding isocyanates.

Scheme 1. Synthesis of 3-Aminobenoisoxazoles[a]

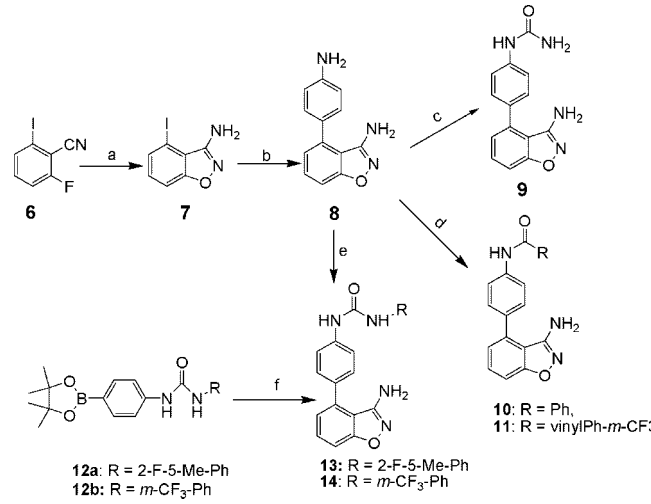

[a] Reagents and conditions: (a) acetohydroxamic acid, *t*-BuOK, DMF, rt; (b) 4-(4,4,5,5-tetramethyl-[1,3,2]dioxaborolan-2-yl)-phenylamine, $PdCl_2$·dppf·CH_2Cl_2, Na_2CO_3, DME, H_2O, 85 °C; (c) acetic acid, NaOCN; (d) RCOCl, pyridine, DMF; (e) RNCO, CH_2Cl_2; (f) **7**, $PdCl_2$·dppf·CH_2Cl_2, Na_2CO_3, DME, H_2O, 85 °C.

3-Aminobenzoisothiazoles were synthesized as illustrated in Scheme 2. Compound **6** was converted to benzylthioether **15** by displacement of the fluoride with phenylmethanethiol. Sequential treatment of **15** with SO_2Cl_2 and ammonia generated the intermediate **16**, which then underwent cyclization in the presence of lithium methoxide to afford 3-aminobenzoisothiazole **17**. Compounds **18** and **19** were obtained via Suzuki coupling reactions of **17** with urea boronates **12a**,**b**. 7-Substituted 3-aminobenzoisoxazoles **49**–**57** were prepared from the previously reported intermediates **46a**−**f**,[35] following the procedures described in Scheme 3.

Results and Discussion

Compounds were assayed against a panel of enzymes including KDR, KIT, and FLT3. The measurements were

Scheme 2. Synthesis of 3-Aminobenzoisothiazoles[a]

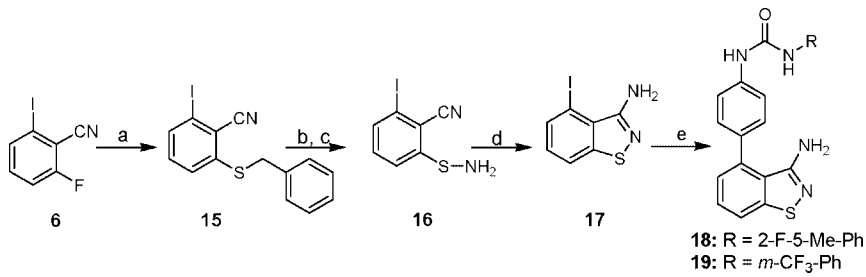

[a] Reagents and conditions: (a) *t*-BuOK, $PhCH_2SH$, DMF; (b) SO_2Cl_2; (c) 7 M NH_3 in MeOH; (d) LiOMe, MeOH; (e) **12**, $PdCl_2 \cdot dppf \cdot CH_2Cl_2$, Na_2CO_3, DME, H_2O.

Scheme 3. Synthesis of 7-Substituted 3-Aminobenzoisoxazoles[a]

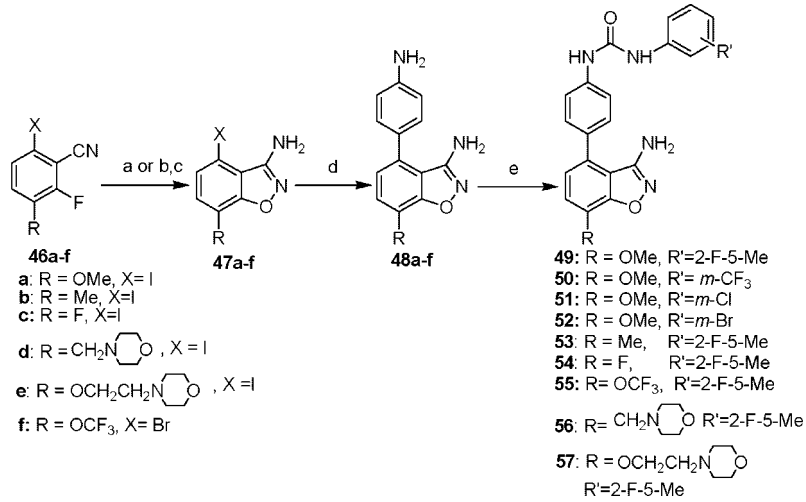

[a] Reagents and conditions: (a) for **47a**−**e**, acetohydroxamic acid, *t*-BuOK, DMF, rt; (b) for **47f**, acetone oxime, *t*-BuOK, THF; (c) 5% HCl, EtOH; (d) 4-(4,4,5,5-tetramethyl-[1,3,2]dioxaborolan-2-yl)-phenylamine, $PdCl_2 \cdot dppf \cdot CH_2Cl_2$, Na_2CO_3, DME, H_2O, 85 °C; (e) RNCO, CH_2Cl_2.

conducted in the presence of a physiologically relevant concentration of adenosine 5′-triphosphate (ATP, 1.0 mM), as previously described.[32] As KDR plays a central role in angiogenesis, structural optimization was primarily focused on KDR. A brief SAR summary is shown in Table 1. As observed in the 3-aminoindazole series,[35] the *N*,*N*′-diphenyl urea moiety was found to be essential for potency in the aminobenzoisoxazole and aminobenzoisothiazole series. This suggests that these compounds exhibit similar binding modes with the enzyme, with the amino and its adjacent ring nitrogen forming hydrogen bonds with KDR hinge region, and the diaryl urea moiety extending into the hydrophobic back pocket of the kinase domain, as shown in Figure 2. Replacement of endocyclic indazole NH-1 with oxygen led to a 5-fold loss of potency (**13** vs **3**), whereas the replacement of NH-1 with sulfur resulted in a 157-fold loss of potency (**18** vs **3**). In general, 3-aminobenzoisoxazole derivatives exhibited improved potency when compared with the related 3-aminobenzoisothiazole compounds (**13** vs **18** and **14** vs **19**).

In an attempt to better understand the SAR trends described above, we studied the intrinsic properties of the three heterocyclic structures, aminoindazole (**20**), aminobenzoisoxazole (**21**), and aminobenzoisothiazole (**22**), in greater detail (Table 2). The binding mode of aminoindazole (**20**) has previously been described as possessing a hydrogen bond donation from the exocyclic N-H(b) to a protein backbone carbonyl and possessing a hydrogen bond accepting interaction to the ring nitrogen N(a) from a protein backbone amide N-H (positions identified in Table 2). Therefore, we calculated the hydrogen bond energies of these two positions as well as the basicity (pK_a) of the ring nitrogen N(a). Relative to aminoindazole (**20**), aminobenzoixazole (**21**) shows decreased basicity, lower hydrogen bond accepting potential at N(a), and increased hydrogen bond donating potential at N(b). The aminobenzoisothiazole (**22**) shows increased basicity, unchanged hydrogen bond accepting potential, and increased hydrogen bond donation potential. The higher electronegativity of oxygen and lower electronegativity of sulfur, relative to nitrogen, provides a rationalization for these calculated observations. In addition to these electronic effects, the larger sulfur atom has the potential to perturb the hinge interactions away from optimal geometry relative to the smaller oxygen and nitrogen atoms. The significant decrease in potency of the aminobenzoisothiazole series, relative to the aminoindazole and aminobenzisoxazole series, is likely due to a combination of the electronic and steric effects noted here. A complete understanding of the relative contributions of these effects will require further study.

Having demonstrated the importance of the *N*,*N*′-diphenyl urea moiety, we then focused on optimization of the terminal phenyl ring of the urea. The effects of *ortho*-, *meta*-, and *para*-substitution and disubstitution on potency were investigated. Several trends can be observed from Table 3. *ortho*-Substitution (cf. **24**–**26**) is not tolerated; even a small group such as fluoro causes a large drop in potency. The detrimental effect of *ortho*-substitution in this series is more significant than in the aminoindazole series.[35] On the other hand, consistent with the aminoindazole series, a variety of *meta*-substituents, including both electron-donating and electron-withdrawing groups (cf. **14**, **27**–**32**) are tolerated, with the *m*-methyl compound **27** providing an approximate 3-fold boost in potency. Substitution at the *para*-

Table 1. Inhibitory Activity of Aminobenzoisoxazoles and Aminobenzoisothiazoles

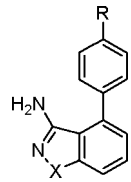

Compd	X	R	KDR IC50 (nM)[a]	KIT IC50 (nM)[a]	FLT3 IC50 (nM)[a]
8	O	NH_2	18,840	14,800	68
9	O	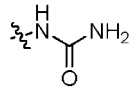	12,500	4,443	619
10	O	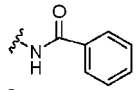	>12,500	>12,500	>12,500
11	O	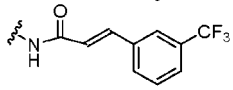	>12,500	>12,500	1,400
13	O	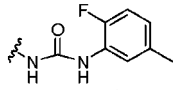	21	23	22
14	O	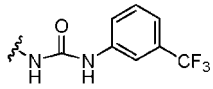	37	114	64
18	S	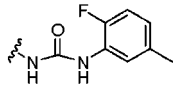	628	790	1,500
19	S	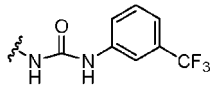	247	2,630	1,260
3	NH	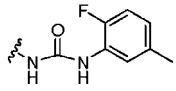	4	16	5

[a] Each IC_{50} determination was performed with seven concentrations, and each assay point was determined in duplicate.

Table 2. pK_a and Hydrogen Bond Parameters in Three Pharmacophores

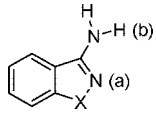

			H-bond parameter ΔE, kcal/mol[b]	
compd	X	pK_a[a]	acceptor N(a)	donor H(b)
20	NH	3.72	10.8	2.60
21	O	2.04	9.60	3.40
22	S	6.04	10.6	3.30

[a] pK values were calculated using ACD/pK_a software (version 10.05, Advanced Chemistry Development Inc., Toronto, ON). [b] Hydrogen bond energies were calculated by using gas phase energies at the Hartree–Fock 6-31G* level. The energy refers to the energy released upon formation of a hydrogen bonded complex between the heterocycle and hydrogen fluoride (HF) by either hydrogen bond donation to the fluoride of HF or hydrogen bond accepting interaction from the hydrogen of HF. Larger values correspond to stronger hydrogen bonds.

position does not significantly affect KDR enzymatic inhibitory activity, however, the KDR cellular activity is diminished (cf. **33**–**37**). Disubstitution is generally well tolerated (cf. **13**, **38**–**45**), with the 3,5-dimethyl compound **38** being the most potent, exhibiting both enzymatic and cellular KDR inhibitory activity of less than 10 nM. Interestingly, addition of a methyl on the *o*-F compound **24** results in an approximate 40-fold boost in cellular potency (cf. **13**), overcoming the deleterious effect of *ortho*-substitution.

Table 3. Inhibitory Activity of Aminobenzoisoxazole Urea Analogs

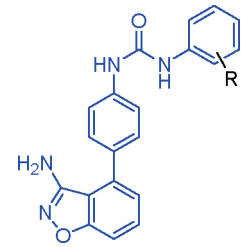

compds	R	KDR IC_{50}[a] (nM)	KIT IC_{50}[a] (nM)	FLT3 IC_{50}[a] (nM)	KDR Cell IC_{50}[b] (nM)
23	H	23	18	7	25
24	*o*-F	318	21	8	497
25	*o*-OCF_3	806	166	60	1000
26	*o*-CF_3	6161	23440	1570	NA
27	*m*-Me	7	12	14	5
28	*m*-OMe	17	4	NA	11
14	*m*-CF_3	37	114	64	65
29	*m*-NO_2	19	14	5	17
30	*m*-F	44	11	NA	21
31	*m*-Br	10	7	NA	5
32	*m*-Cl	8	10	6	28
33	*p*-CH_3	16	5	4	44
34	*p*-CF_3	32	27	NA	173
35	*p*-OMe	22	5	NA	106
36	*p*-F	134	7	4	23
37	*p*-OCF_3	42	102	27	123
13	2-F-5-Me	21	23	22	13
38	3,5-di-Me	8	37	17	3
39	2-F-5-CF_3	104	339	213	80
40	3-F-4-Me	15	12	NA	40
41	3-CF_3-4-F	23	62	28	94
42	3-Cl-4-F	59	36	22	19
43	3,5-di-F	67	14	NA	81
44	3-Cl-4-OMe	8	24	8	36
45	3-Cl-4-Me	8	50	37	32

[a] Each IC_{50} determination was performed with seven concentrations, and each assay point was determined in duplicate. [b] Each cellular IC_{50} determination was performed with five concentrations, and each assay point was determined in duplicate.

As the binding modes of 3-aminobenzoisoxazoles and 3-aminoindazoles are similar, substituents at the C7 position in the 3-aminobenzoisoxazole series would be expected to project toward solvent.[35] Thus, we further investigated the effect of C7 substitution, including groups that might improve aqueous solubility. As shown in Table 4, electron-donating groups such as methoxy, methyl, are tolerated (cf. **49**−**53**); in contrast, electron-withdrawing groups such as fluoro and trifluoromethoxy are detrimental to potency (cf. **54**, **55**). Installation of the water solubilizing morpholine group linked by a two-carbon ether tether led to retention of both enzymatic and cellular potency (cf. **57**).

Select compounds were further evaluated for their selectivity against other tyrosine kinases. As shown in Table 5, the compounds potently inhibited all members of the VEGR and PDGFR families and exhibited modest inhibitory activity against Tie-2, but were selective over other nonstructurally related tyrosine kinases such as FGFR, HCK, SRC, and LYN.

Compounds with promising in vitro enzymatic and cellular inhibitory activity were further evaluated for their pharmacokinetic properties in mice. Data for **3** are included for comparison. As shown in Table 6, the 2-F-5-Me phenyl urea analog **49** had the lowest oral bioavailability (34%), however, all other analogs incorporating halo or trifluoromethyl substituents had very high levels of oral bioavailability that are comparable to

Table 4. Inhibitory Activity of 7-Substituted Benzoisoxazole Urea Analogs

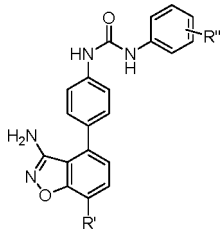

Compd	R'	R''	KDR IC_{50} (nM)[a]	KIT IC_{50} (nM)[a]	FLT3 IC_{50} (nM)[a]	KDR Cell IC_{50} (nM)[b]
13	H	2-F-5-Me	21	23	22	13
49	OMe	2-F-5-Me	21	43	36	20
50	OMe	*m*-CF_3	11	56	19	31
51	OMe	*m*-Cl	41	72	30	18
52	OMe	*m*-Br	8	23	16	15
53	Me	2-F-5-Me	71	64	61	39
54	F	2-F-5-Me	211	216	173	NA
55	OCF_3	2-F-5-Me	158	294	58	179
56	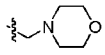	2-F-5-Me	365	114	82	NA
57	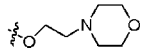	2-F-5-Me	45	71	34	22

[a] Each IC_{50} determination was performed with seven concentrations, and each assay point was determined in duplicate. [b] Each cellular IC_{50} determination was performed with five concentrations, and each assay point was determined in duplicate.

3. In general, the compounds were characterized by moderate volume of distribution (V_d) and low clearance.

Acute in vivo efficacy was assessed using the estradiol-induced murine uterine edema (UE) assay, an in vivo model of VEGF-stimulated vascular permeability. As seen in Table 7, a number of compounds displayed excellent efficacy in this model after oral adminisration (ED_{50} < 10 mg/kg). Compounds that showed efficacy in the uterine edema model and possessed favorable PK profiles were evaluated in the human fibrosarcoma HT1080 xenograft tumor growth model. Several compounds exhibited significant inhibition of tumor growth. In particular, compound **50** displayed 81% inhibition at 10 mg/kg/day (Figure 4), which is more potent on a dose basis than **3** in this model.[37] Furthermore, the cardiac safety of inhibitors **49** and **50** were evaluated using a [^{3}H] dofetilide binding assay, a predictive screening tool for hERG blockade. Both **49** and **50** showed low affinity with an IC_{50} value greater than 30 uM.

Conclusion

By substituting the NH-1 of the 3-aminoindazole series with oxygen, we have developed a novel series of 3-aminobenzoisoxazole *N*,*N*′-diphenyl urea derivatives as multitargeted RTK inhibitors that potently inhibit both VEGFR and PDGFR family members. Optimization of the urea moiety and substitution at 7-position led to several compounds that displayed high oral bioavailability and excellent in vivo efficacy in the estradiol-induced murine uterine edema (UE) assay and HT1080 tumor growth inhibition model. In particular, compound **50** shows high oral bioavailability and improved antitumor efficacy in the human fibrosarcoma (HT1080) model relative to **3**.

Experimental Section

HTRF Assays of Receptor Tyrosine Kinases. Assays were performed in a total of 40 μL in 96-well Costar black half-volume plates using HTRF technology. Peptide substrate (Biotin-Ahx-AEEEYFFLFA-amide) at 4 μM, 1 mM ATP, enzyme, and inhibitors were incubated for 1 h at ambient temperature in 50 mM Hepes/NaOH, pH 7.5, 10 mM $MgCl_2$, 2 mM $MnCl_2$, 2.5 mM DTT, 0.1 mM orthovanadate, and 0.01% BSA. Inhibitors were added to the wells at final concentrations of 3.2 nM to 50 μM with 5% DMSO added as cosolvent. The reactions were stopped with 10 μL/well 0.5 M EDTA and then 75 μL of buffer containing streptavidin-allophycocyanin (Prozyme; 1.1 μg/mL) and PT66 antibody Europium cryptate (Cis-Bio; 0.1 μg/mL) was added to each well. The plates were read from 1 to 4 h after addition of the detection reagents and the time-resolved fluorescence (665 to 615 ratio) measured using a Packard Discovery instrument. The amount of each tyrosine kinase added to the wells was calibrated to give a control (no inhibitor) to background (prequenched with EDTA) ratio of 10–15 and was shown to be in the low nanomolar concentration range for each kinase. The inhibition of each well was calculated using the control and background readings for that plate. KDR, CSF1R, KIT, FLT1, and FLT3 were assayed using the above protocol. The HTRF detection was done in the same way as for the other kinases. Inhibition constants are the mean of two determinations performed with seven concentrations of the test compounds.

Cellular KDR Phosphorylation Assay Determined by ELISA. NIH3T3 cells stably transfected with full length human KDR (VEGFR2) were maintained in DMEM medium with 10% fetal bovine serum and 500 μg/mL geneticin. KDR cells were plated at 20000 cells/well into duplicate 96-well tissue culture plates and cultured overnight in an incubator at 37 °C with 5% CO_2 and 80% humidity. The growth medium was replaced with serum-free growth medium for 2 h prior to compound addition. Compounds in DMSO were diluted in serum-free growth medium (final DMSO concentration 1%) and added to cells for 20 min prior to stimulation for 10 min with VEGF (50 ng/mL). Cells were lysed by addition of RIPA buffer (50 mM Tris-HCl (pH 7.4), 1% IGEPAL, 150 mM NaCl, 1 mM EDTA, and 0.25% sodium deoxycholate) containing protease inhibitors (Sigma cocktail), NaF (1 mM), and Na_3VO_4 (1 mM) and placed on a microtiter plate shaker for 10 min. The lysates from duplicate wells were combined, and 170 μL of the combined lysate was added to the KDR ELISA plate. The KDR ELISA plate was prepared by adding anti-VEGFR2 antibody (1 μg/well, R&D Systems) to an unblocked plate and incubated overnight at 4 °C. The plate was then blocked for at least 1 h with 200 μL/well of 5% dry milk in PBS. The plate was washed two times with PBS containing 0.1% Tween 20 (PBST) before addition of the cell lysates. Cell lysates were incubated in the KDR ELISA plate with constant shaking on a microtiter plate shaker for 2 h at room temperature. The cell lysate was then removed and the plate was washed five times with PBST. Detection of phospho-KDR was performed using a 1:2000 dilution of biotinylated 4G10 antiphosphotyrosine (UBI, Lake Placid, NY), incubated with constant shaking for 1.5 h at room temperature, and washed five times with PBST, and for detection, a 1:2000 dilution of strepavidin-HRP (UBI, Lake Placid, NY) was added and incubated with constant shaking for 1 h at room temperature. The wells were then washed five times with PBST and K-Blue HRP ELISA substrate (Neogen) was added to each well. Development time was monitored at 650 nm in a SprectrMax Plus plate reader until 0.4–0.5 absorbance units were obtained (approximately 10 min) in the VEGF only wells. Phosphoric acid (1 M) was added to stop the reaction, and the plate was read at 450 nm. Percent inhibition was calculated using the VEGF only wells as 100% controls and wells containing 5 μM pan-kinase inhibitor as 0% controls (no VEGF wells were used to monitor endogenous phosphorylation state of the cells). IC_{50} values were calculated by nonlinear regression analysis of the concentra-

Table 5. Kinase Inhibition Profiles of Selected Compounds[a]

	VEGFR IC_{50} (nM)		PDGFR IC_{50} (nM)				other kinases IC_{50} (nM)				
compd	KDR	FLT1	FLT3	KIT	CSF1R	PDGFR-β	TIE-2	FGFR	HCK	SRC	LYN
49	21	24	36	43	27	96	249	NA	>50000	>50000	>50000
50	11	16	19	56	30	130	270	3000	>50000	>50000	>50000
51	41	38	30	72	40	NA	1000	NA	>50000	>50000	>50000
3	4	3	4	14	3	66	170	>12500	>50000	>50000	>50000

[a] Each IC_{50} determination was performed with seven concentrations, and each assay point was determined in duplicate.

Table 6. Mouse Pharmacokinetic Parameters of Selected Compounds

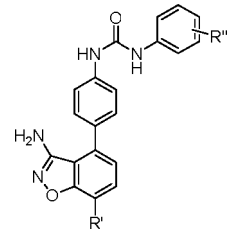

			IV				PO[a]	
compd	R′	R″	dose (mg/kg)	$t_{1/2}$ (h)	V_d (L/Kg)	CL (L/hr·kg)	F (%)	AUC (μM·h)
41	H	3-CF_3-4-F	3	1.2	1.4	0.79	100	33.1
49	OMe	2-F-5-Me	3	0.66	0.94	1.0	34	8.5
50	OMe	3-CF3	1	0.9	2.2	1.7	100	30.6
51	OMe	3-Cl	1	0.9	1.2	0.93	99	25.8
52	OMe	3-Br	3	1.9	3.1	1.1	71	13.8
3			3	1.7	2.7	1.1	100	24.5

[a] Dose orally at 10 mg/kg.

Table 7. In Vivo Efficacy in Murine Uterine Edema Model and Antitumor Efficacy in HT1080 Model

compd	UE ED_{50} (mg/kg)	HT1080 TGI (PI 2g)[a]
41	5.4	63% @ 30 mg/kg/day[b]
49	3.2	55% @ 30 mg/kg/day[b]
50	2.0	81% @ 10 mg/kg/day[b]
51	90% @ 3 mg/kg	45% @ 30 mg/kg/day[b]
52	1.0	ND
3	0.4	69% @ 10 mg/kg/day[b]

[a] PI: percent inhibition of tumor growth relative to control at 2 g. [b] Compounds were dosed twice daily (BID).

tion–response curve. Each IC_{50} determination was performed with five concentrations and each assay point was determined in duplicate.

Estradiol-Induced Murine Uterine Edema Assay. Female Balb/C mice greater than twelve weeks old (Taconic, Germantown, NY) were pretreated with 10 units of Pregnant Mare's Serum Gonadotropin (PMSG; Calbiochem) at 72 and 24 h prior to compound administration (0.1 mL/mouse IP). Mice were randomized the day of the experiment. Test compounds were formulated in a variety of vehicles and administered p.o. 30 min prior to stimulation with an i.p. injection of water-soluble 17β-estradiol (20–25 μg/mouse). Animals were sacrificed and the uteri were removed 2.5 h following estradiol stimulation by cutting just proximal to the cervix and at the fallopian tubes. After removal of fat and connective tissue, uteri were weighed, squeezed between filter paper to remove fluid, and weighed again. The difference between wet and blotted weights represented the fluid content of the uterus. Compound-treated groups were compared to vehicle-treated animals after subtracting the background water content of unstimulated uteri. Experimental group size was 5 or 6.

HT1080 Tumor Growth Inhibition Model. A total of 1080 human fibrosarcoma cells were obtained from the American type Tissue Culture Collection and maintained in Dulbecco's Modified Eagle Medium supplemented with 10% fetal bovine serum and antibiotics. For tumor xenograft studies, cells were suspended in PBS, mixed with an equal volume of Matrigel (phenol red free) to a final concentration of 2 million cells/mL, and inoculated (0.25 mL) into the flank of SCID-Beige mice. One week after inoculation, tumor bearing animals were divided into groups (n = 10) and administration of vehicle (2% EtOH, 5% Tween80, 20% PEG400, 73% saline) or inhibitor at the indicated dose was initiated. Tumor growth was assessed every 2–3 days by measuring tumor size and calculating tumor volume using the formula [length × width^2]/2.

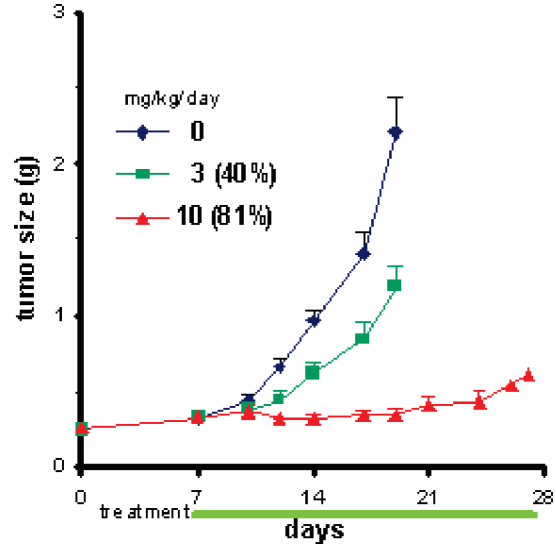

Figure 4. Effects of inhibitor **50** on the growth of HT1080 human xenograft, dosing twice daily (BID) started on day 7. Tumor volumes are expressed as mean ± SEM, n = 10 per group. Significant differences (p > 0.05 vs control) in mean tumor volume were observed for all treatment groups by day 14. Total daily dose (mg/kg/day) and percent inhibition of control (2 g) are indicated in the legend.

[^{3}H] Dofetilide/HEK-293 Membrane Competition Binding Assay. The affinity of test drugs for the hERG cardiac K^+ channel was determined by their ability to displace tritiated dofetilide (a class III antiarrhythmic drug and potent hERG blocker) in membrane homogenates from HEK-293 cells heterogeneously

expressing the hERG cannel. Drug dilutions were prepared from 10 mM DMSO stocks, and the following were added to a 96-well polystyrene plate (Perkin-Elmer Optiplate): 20 μL of assay binding buffer (for total bounds), 1 μM astemizole (for nonspecific bounds), or test drug, 50 μL of [3H]dofetilide (20 nM, 85 Ci/mmol specific activity), and 130 μL of membrane homogenate (final protein concentration of 30 μg per well). This plate was incubated at ambient temperature for 45 min, aspirated onto GF/B filter plates (Perkin-Elmer), and washed with 2 mL of cold wash buffer. After allowing the plates to dry, 50 μL of scintillant (Perkin-Elmer MicroScint 20) was added to each well, and the radioactivity was counted in a Perkin-Elmer Topcount NXT scintillant counter. TC_{50} determinations were calculated from competition curves using six drug concentrations, half-log apart, starting at a high concentration of 100 μL (final assay DMSO concentration = 1%) using a four-parameter logistic equation.

Chemistry. ^{1}H NMR spectra were recorded on a 300 MHz or a 500 MHz (GE QE 300 or QE 500) spectrometer and chemical shifts are reported in parts per million (ppm, δ) relative to tetramethylsilane as an internal standard. Mass spectra were obtained on a Finnigan MAT SSQ700 instrument. Elemental analysis (C, H, N) was performed by Robertson Microlit Laboratories, Inc., Madison, WI. Silica gel 60 (E. Merck, 230–400 mesh) was used for preparative column chromatography.

4-Iodo-benzo[*d*]isoxazol-3-ylamine (7). *t*-BuOK (4.72 g, 42.1 mmol) was added to a solution of acetohydroxamic acid (3.16 g, 42.1 mmol) in DMF (50 mL). The mixture was stirred at room temperature for 30 min, and then 2-fluoro-6-iodo-benzonitrile (5.2 g, 21.05 mmol) was added. The reaction mixture was stirred for an additional 10 h, then diluted with water (300 mL), and filtered. The solid was rinsed with water and dried to provide the title compound as a white solid (3.65 g, 67%). ^{1}H NMR (DMSO-d_6) δ 5.92 (s, 2 H), 7.21 – 7.31 (m, 1 H), 7.55 (d, J = 8.48 Hz, 1 H), 7.70 (d, J = 7.46 Hz, 1 H). MS (ESI) m/z 261 $(M + H)^+$.

4-(4-Aminophenyl)-benzo[*d*]isoxazol-3-ylamine (8). A mixture of compound **7**, (585 mg, 2.25 mol), 4-(4,4,5,5-tetramethyl [1,3,2]-dioxaborolan-2-yl)-phenylamine (591 mg, 2.7 mol), $Pd(PPh_3)_4$ (260 mg, 0.225 mol), and Na_2CO_3 (596 mg, 5.6 mmol) in DME (40 mL) and water (10 mL) was degassed with nitrogen, then heated to 85 °C for 4 h. The reaction mixture was cooled to room temperature and partitioned between ethyl acetate and water. The aqueous layer was extracted with ethyl acetate. The combined extracts were washed with water and brine, dried ($MgSO_4$), filtered, and concentrated to dryness. The crude product was purified by flash column chromatography on silica gel with 0–5% MeOH in CH_2Cl_2 to afford the title compound as a light tan solid (300 mg, 59%). ^{1}H NMR (DMSO-d_6) δ 5.21 (s, 2 H), 5.39 (s, 2 H), 6.70 (d, J = 8.14 Hz, 2 H), 7.05 (d, J = 6.78 Hz, 1 H), 7.16 (d, J = 8.14 Hz, 2 H), 7.39 (d, J = 8.14 Hz, 1 H), 7.52 (t, J = 7.80 Hz, 1 H). MS (ESI) m/z 226 $(M + H)^+$. Anal. ($C_{13}H_{11}N_3O$) C, H, N.

1-(4-(3-Aminobenzo[*d*]isoxazol-4-yl)phenyl)urea (9). Compound **8** (45 mg, 0.2 mmol) and NaOCN (26 mg, 0.4 mmol) were suspended in acetic acid (1 mL) and water (1 mL). The reaction mixture was stirred at room temperature for 10 h, then poured into water (20 mL). The resulting solid was collected by filtration. The crude product was recrystallized from THF and hexane to afford the title compound as an off-white solid (35 mg, 65%). ^{1}H NMR (DMSO-d_6) δ 5.20 (s, 2 H), 5.92 (s, 2 H), 7.11 (d, J = 7.12 Hz, 1 H), 7.30–7.40 (m, 2 H), 7.42–7.50 (m, 1 H), 7.53–7.64 (m, 3 H), 8.72 (s, 1 H). MS (ESI) m/z 269 $(M + H)^+$. Anal. ($C_{14}H_{12}N_4O_2$) C, H, N.

***N*-[4-(3-Aminobenzo[*d*]isoxazol-4-yl)-phenyl]-benzamide (10).** To a solution of compound **8** (45 mg, 0.2 moml) in DMF (2 mL) was added pyridine (19 μL, 0.24mmol), followed by benzoyl chloride (23.2 μL, 0.2 mmol). The mixture was stirred at room temperature for 3 h, then partitioned between water and ethyl acetate. The aqueous layer was extracted with ethyl acetate, and the combined extracts were washed with water and brine, dried ($MgSO_4$), filtered, and concentrated to dryness. The crude product was purified by flash column chromatography on silica gel, eluting with 0–4% MeOH in CH_2Cl_2 to afford the title compound as a white solid (42 mg, 64%). ^{1}H NMR (DMSO-d_6) δ 5.22 (s, 2 H), 7.09–7.23 (m, 1 H), 7.44–7.68 (m, 7 H), 7.88–8.06 (m, 4 H), 10.20–10.56 (m, 1 H). MS (ESI) m/z 330 $(M + H)^+$. Anal. ($C_{20}H_{15}N_3O_2$) C, H, N.

***N*-[4-(3-Aminobenzo[*d*]isoxazol-4-yl)-phenyl]-3-(3-trifluoromethyl-phenyl)-acrylamide (11).** Compound **11** was prepared using the same procedure described for the synthesis of **10**, substituting *trans*-3-(trifluromethyl)cinnamoyl chloride for benzoyl chloride. ^{1}H NMR (DMSO-d_6) δ 5.22 (s, 2 H), 7.01 (d, J = 15.94 Hz, 1 H), 7.16 (m, 1 H), 7.45–8.09 (m, 11 H), 10.45 (s, 1 H). MS (ESI) m/z 424 $(M + H)^+$. Anal.($C_{23}H_{16}F_3N_3O_2$) C, H, N.

1-(2-Fluoro-5-methylphenyl)-3-(4-(4,4,5,5-tetramethyl-1,3,2-dioxaborolan-2-yl)phenyl)urea (12a). To a solution of 4-(4,4,5,5-tetramethyl-1,3,2-dioxaborolan-2-yl)aniline (219 mg, 1mmol) in dichloromethane (5 mL) was added dropwise 2-fluoro-5-methylphenyl isocyanate (151 mg, 1 mmol). The mixture was stirred at room temperature for 10 h. The solid was collected by filtration to afford the title compound as a white solid (330 mg, 89%). ^{1}H NMR (DMSO-d_6) δ 1.28 (s, 12 H), 2.27 (s, 3 H), 6.49–6.90 (m, 1 H), 7.10 (dd, J = 11.53, 8.48 Hz, 1 H), 7.47 (d, J = 8.48 Hz, 2 H), 7.53–7.65 (m, 2 H), 7.98 (dd, J = 7.97, 1.86 Hz, 1 H), 8.51 (d, J = 1.70 Hz, 1 H), 9.19 (s, 1 H). MS (ESI) m/z 371 $(M + 1)^+$.

1-(4-(4,4,5,5-Tetramethyl-1,3,2-dioxaborolan-2-yl)phenyl)-3-(3(trifluoromethyl)-phenyl)urea (12b). Compound **12b** was prepared using the same procedure described for the synthesis of **12a**, substituting 3-(trifluoromethyl)phenyl isocyanate for 2-fluoro-5-methylphenyl isocyanate. ^{1}H NMR (DMSO-d_6) δ 1.29 (s, 12 H), 7.32 (d, J = 7.12 Hz, 1 H), 7.42 – 7.66 (m, 6 H), 8.03 (s, 1 H), 8.94 (s, 1 H), 9.07 (s, 1 H). MS (ESI) m/z 407 $(M + 1)^+$.

1-(4-(3-Aminobenzo[*d*]isoxazol-4-yl)phenyl)-3-(2-fluoro-5-methylphenyl)urea (13). Method A. A mixture of compound **7** (52 mg, 0.2 mmol), compound **12a** (81 mg, 0.22 mmol), Na_2CO_3 (64 mg, 0.6 mmol) and $PdCl_2(dppf)\cdot CH_2Cl_2$ (8.2 mg, 0.01mmol) in DME (4 mL) and water (1 mL) were degassed with nitrogen, then heated to 85 °C for 4 h. The reaction mixture was cooled to room temperature and partitioned between ethyl acetate and water. The aqueous layer was extracted with ethyl acetate. The combined extracts were washed with water and brine, dried ($MgSO_4$), filtered, and concentrated to dryness. The crude product was purified by flash column chromatography on silica gel with 0–5% MeOH in CH_2Cl_2 to afford the title compound (38 mg, 50%).

Method B. A solution of compound **8** (45 mg, 0.2 mol) in CH_2Cl_2 (2 mL) was cooled to 0 °C, and then 2-fluoro-5-methylphenyl isocyanate (30 mg, 0.2 mmol) was added dropwise. The mixture was stirred at 0 °C for 1 h and then at room temperature for 10 h. The resulting white suspension was filtered, affording the title compound as a white solid (49 mg, 65%). ^{1}H NMR (DMSO-d_6) δ 2.28 (s, 3 H), 5.22 (s, 2 H), 6.75–6.85 (m, 1 H), 7.06–7.18(m, 2 H), 7.40–7.66 (m, 6 H), 8.00 (dd, J = 7.97, 1.86 Hz, 1 H), 8.55 (d, J = 2.37 Hz, 1 H), 9.25 (s, 1 H). MS (ESI) m/z 377 $(M + H)^+$. Anal. ($C_{21}H_{17}FN_4O_2$) C, H, N.

1-(4-(3-Aminobenzo[*d*]isoxazol-4-yl)phenyl)-3-(3-(trifluoromethyl)phenyl)urea (14). Compound **14** was prepared using the same procedure described for the synthesis of **13** (method A) by substituting **12b** for **12a**. ^{1}H NMR (DMSO-d_6) δ 5.22 (s, 2 H), 7.14 (d, J = 6.78 Hz, 1 H), 7.33 (d, J = 7.12 Hz, 1 H), 7.40–7.75 (m, 8 H), 8.04 (s, 1 H), 9.00 (s, 1 H), 9.12 (s, 1 H). MS (ESI) m/z 413 $(M + H)^+$. Anal. ($C_{21}H_{15}F_3N_4O_2$) C, H, N.

2-(Benzylthio)-6-iodobenzonitrile (15). Benzyl mercaptan (2.36 mL, 20 mmol) was added to a suspension of *t*-BuOK (2.69 g, 24 mmol) in anhydrous DMF (100 mL). The mixture was stirred at room temperature for 10 min, and then 2-fluoro-6-iodo-benzonitrile (4.94 g, 20 momol) was added. Stirring was continued for 3 h and then the reaction mixture was poured into water (1 L). Upon stirring a yellow precipitate was formed. This solid was collected by filtration and rinsed with water. The crude product was stirred in hot hexane, then cooled to room temperature, and filtered to collect the title compound as a yellow solid (6.0 g, 85%). ^{1}H NMR (DMSO-d_6) δ 4.40 (s, 2 H), 7.19–7.46 (m, 6 H), 7.61 (d, J = 7.12 Hz, 1 H) 7.81 (d, J = 8.81 Hz, 1 H). MS (ESI) m/z 350 $(M - H)^-$.

2-(Aminothio)-6-iodobenzonitrile (16). Compound **15** (1.76 g, 5 mmol) was dissolved in CH_2Cl_2 (10 mL) and SO_2Cl_2 (0.49 mL, 6 mmol) was added. The mixture was stirred at room temperature for 10 h and then concentrated to dryness. To the residue was added 7 M NH_3 in MeOH (20 mL). The mixture was stirred 2 h at room temperature, then diluted with water, extracted with ethyl acetate, washed with brine, dried ($MgSO_4$), and concentrated to dryness. The residue was dissolved in a minimum amount of ethyl acetate and reprecipitated with hexane. The resulting solid was collected by filtration to afford the title compound as a light tan solid. (0.75 g, 54%). ^{1}H NMR (DMSO-d_6) δ 4.43 (s, 2 H), 7.34–7.46 (m, 1 H), 7.64 (d, J = 7.12 Hz, 1 H), 7.70 (d, J = 7.80 Hz, 1 H). MS (ESI) m/z 277 $(M + H)^+$.

4-Iodobenzo[*d*]isothiazol-3-amine (17). To a solution of compound **16** (700 mg, 2.54 mmol) in methanol (10 mL) was added 1 M LiOMe methanol solution (3 mL, 3 mmol). The reaction mixture was heated to 70 °C for 1 h and then cooled to room temperature. The resulting solid was collected by filtration to afford the title compound as a light tan solid (408 mg, 58%) ^{1}H NMR (DMSO-d_6) δ 6.50 (s, 2 H), 7.12–7.24 (m, 1 H), 7.92 (d, J = 8.14 Hz, 1 H), 8.03 (d, J = 8.14 Hz, 1 H). MS (ESI) m/z 277 $(M + H)^+$.

1-(4-(3-Aminobenzo[*d*]isothiazol-4-yl)phenyl)-3-(2-fluoro-5-methylphenyl)urea (18). A mixture of compound **17** (55 mg, 0.2 mmol), **12a** (81 mg, 0.22 mmol), and $PdCl_2(dppf)\cdot CH_2Cl_2$ (16 mg, 0.02 mmol) in DME (2 mL) was degassed with nitrogen and then a solution of Na_2CO_3 (64 mg, 0.6 mmol) in water (1 mL) was added. The mixture was heated to 80 °C for 4 h. After cooling to room temperature, the reaction mixture was extracted with ethyl acetate, washed with water and brine, dried ($MgSO_4$), filtered, and concentrated to dryness. The crude product was purified by flash column chromatography on silica gel with 0–2% MeOH in CH_2Cl_2 to afford the title compound (40 mg, 51%).^{1}H NMR (DMSO-d_6) δ 2.28 (s, 3 H), 5.45 (s, 2 H), 6.69–6.92 (m, 1 H), 7.02–7.24 (m, 2 H), 7.37 (d, J = 8.48 Hz, 2 H), 7.49–7.59 (m, 1 H), 7.62 (d, J = 8.48 Hz, 2 H), 7.88–8.08 (m, 2 H), 8.56 (d, J = 2.37 Hz, 1 H), 9.27 (s, 1 H). MS (ESI) m/z 393 $(M + H)^+$. Anal. ($C_{21}H_{17}FN_4OS\cdot 0.4\ CH_3OH\cdot 0.15CH_2Cl_2$).

1-(4-(3-Aminobenzo[*d*]isothiazol-4-yl)phenyl)-3-(3-(trifluoromethyl)phenyl)urea (19). Compound **19** was prepared using the procedure described for the synthesis of compound **18** by substituting compound **12b** for **12a**. ^{1}H NMR (DMSO-d_6) δ 5.45 (s, 2 H), 7.17 (d, J = 6.10 Hz, 1 H), 7.28–7.41 (m, 3 H), 7.48–7.73 (m, 5 H), 7.98 (d, J = 8.14 Hz, 1 H), 8.04 (s, 1 H), 9.02 (s, 1 H), 9.13 (s, 1 H). MS (ESI) m/z 429 $(M + H)^+$. Anal. ($C_{21}H_{15}F_3N_4OS\cdot 0.1CH_2Cl_2$) C, H, N.

Compounds **23**–**45** were prepared using the procedure described for the synthesis of compound **13** (method B), substituting the appropriate isocyanate for 2-fluoro-5-methylphenyl isocyanate.

1-(4-(3-Aminobenzo[*d*]isoxazol-4-yl)phenyl)-3-phenylurea (23). ^{1}H NMR (DMSO-d_6) δ 5.24 (s, 2 H), 7.00 (t, J = 7.17 Hz, 1 H), 7.15 (d, J = 7.32 Hz, 1 H), 7.31 (t, J = 7.78 Hz, 2 H), 7.48 (dd, J = 22.43, 7.78 Hz, 5 H), 7.55–7.71 (m, 3 H), 8.76 (s, 1 H), 8.89 (s, 1 H). MS (ESI) m/z 345 $(M + H)^+$. Anal. ($C_{20}H_{16}N_4O_2\cdot 0.3H_2O$) C, H, N.

1-(4-(3-Aminobenzo[*d*]isoxazol-4-yl)phenyl)-3-(2-fluorophenyl)urea (24). ^{1}H NMR (DMSO-d_6) δ 5.22 (s, 2 H), 6.89–7.08 (m, 1 H), 7.10–7.36 (m, 3 H), 7.39–7.53 (m, 3 H), 7.53–7.72 (m, 3 H), 8.05–8.29 (m, 1 H), 8.62 (d, J = 2.37 Hz, 1 H), 9.27 (s, 1 H). MS (ESI) m/z 363 $(M + H)^+$. Anal. ($C_{20}H_{15}FN_4O_2\cdot 0.1CH_2Cl_2$) C, H, N.

1-(4-(3-Aminobenzo[*d*]isoxazol-4-yl)phenyl)-3-(2-(trifluoromethoxy)phenyl)urea (25). ^{1}H NMR (DMSO-d_6) δ 5.23 (s, 2 H), 6.96–7.23 (m, 2 H), 7.30–7.53 (m, 5 H), 7.54–7.77 (m, 3 H), 8.28 (dd, J = 8.31, 1.53 Hz, 1 H), 8.55 (s, 1 H), 9.48 (s, 1 H). MS (ESI) m/z 429 $(M + H)^+$. Anal. ($C_{21}H_{15}F_3N_4O_3$) C, H, N.

1-(4-(3-Aminobenzo[*d*]isoxazol-4-yl)phenyl)-3-(2-(trifluoromethyl)phenyl)urea (26). ^{1}H NMR (DMSO-d_6) δ 5.22 (s, 2 H), 7.00–7.75 (m, 10 H), 7.95 (d, J = 7.80 Hz, 1 H), 8.16 (s, 1 H), 9.57 (s, 1 H). MS (ESI) m/z 413 $(M + H)^+$. Anal. ($C_{21}H_{15}F_3N_4O_2\cdot 0.35H_2O$) C, H, N.

1-(4-(3-Aminobenzo[*d*]isoxazol-4-yl)phenyl)-3-*m*-tolylurea (27). ^{1}H NMR (DMSO-d_6) δ 2.29 (s, 3 H), 5.22 (s, 2 H), 6.81 (d, J = 7.12 Hz, 1 H), 7.10–7.70 (m, 10 H), 8.66 (s, 1 H), 8.85 (s, 1 H). MS (ESI) m/z 359 $(M + H)^+$. Anal. ($C_{21}H_{18}N_4O_2\cdot 0.4H_2O$) C, H, N.

1-(4-(3-Aminobenzo[*d*]isoxazol-4-yl)phenyl)-3-(3-methoxyphenyl)urea (28). ^{1}H NMR (DMSO-d_6) δ 3.74 (s, 3 H), 5.22 (s, 2 H), 6.57 (dd, J = 7.97, 2.20 Hz, 1 H), 6.85–7.03 (m, 1 H), 7.07–7.29 (m, 3 H), 7.37–7.52 (m, 3 H), 7.53–7.71 (m, 3 H), 8.75 (s, 1 H), 8.86 (s, 1 H). MS (ESI) m/z 376 $(M + H)^+$. Anal. ($C_{21}H_{18}N_4O_3\cdot 0.15H_2O$) C, H, N.

1-(4-(3-Aminobenzo[*d*]isoxazol-4-yl)phenyl)-3-(3-nitrophenyl)urea (29). ^{1}H NMR (DMSO-d_6) δ 5.22 (s, 2 H), 7.15 (d, J = 6.78 Hz, 1 H), 7.48 (t, J = 8.65 Hz, 3 H), 7.54–7.70 (m, 4 H), 7.75 (dd, J = 7.80, 1.70 Hz, 1 H), 7.84 (dd, J = 8.14, 2.37 Hz, 1 H), 8.59 (t, J = 2.20 Hz, 1 H), 9.09 (s, 1 H), 9.34 (s, 1 H). MS (ESI) m/z 390 $(M + H)^+$. Anal. ($C_{20}H_{15}N_5O_4$) C, H, N.

1-(4-(3-Aminobenzo[*d*]isoxazol-4-yl)phenyl)-3-(3-fluorophenyl)urea (30). ^{1}H NMR (DMSO-d_6) δ 5.22 (s, 2 H), 6.75–6.86 (m, 1 H), 7.10–7.20 (m, 2 H), 7.26–7.36 (m, 1 H), 7.41–7.66 (m, 7 H), 8.94 (s, 1 H), 8.98 (s, 1 H). MS (ESI) m/z 363 $(M + H)^+$. Anal. ($C_{20}H_{15}FN_4O_2$) C, H, N.

1-(4-(3-Aminobenzo[*d*]isoxazol-4-yl)phenyl)-3-(3-bromophenyl)urea (31). ^{1}H NMR (DMSO-d_6) δ 5.22 (s, 2 H), 7.16 (t, J = 7.29 Hz, 2 H), 7.25 (t, J = 7.97 Hz, 1 H), 7.30–7.37 (m, 1 H), 7.40–7.52 (m, 3 H), 7.55–7.68 (m, 3 H), 7.88 (t, J = 1.86 Hz, 1 H), 8.95 (s, 1 H), 8.96 (s, 1 H). MS (ESI) m/z 425 $(M + H)^+$. Anal. ($C_{20}H_{15}BrN_4O_2$) C, H, N.

1-(4-(3-Aminobenzo[*d*]isoxazol-4-yl)phenyl)-3-(3-chlorophenyl)urea (32). ^{1}H NMR (DMSO-d_6) δ 5.22 (s, 2 H), 6.96–7.09 (m, 1 H), 7.14 (d, J = 7.12 Hz, 1 H), 7.24–7.38 (m, 2 H), 7.40–7.52 (m, 3 H), 7.54–7.67 (m, 3 H), 7.70–7.77 (m, 1 H), 8.96 (s, 2 H). MS (ESI) m/z 379 $(M + H)^+$. Anal. ($C_{20}H_{15}ClN_4O_2\cdot 0.15H_2O$) C, H, N.

1-(4-(3-Aminobenzo[*d*]Isoxazol-4-yl)phenyl)-3-*p*-tolylurea (33). ^{1}H NMR (DMSO-d_6) δ 2.25 (s, 3 H), 5.22 (s, 2 H), 6.97–7.20 (m, 3 H), 7.30–7.52 (m, 5 H), 7.53–7.69 (m, 3 H), 8.62 (s, 1 H), 8.83 (s, 1 H). MS (ESI) m/z 359 $(M + H)^+$. Anal. ($C_{21}H_{18}N_4O_2\cdot 0.15H_2O$) C, H, N.

1-(4-(3-Aminobenzo[*d*]isoxazol-4-yl)phenyl)-3-(4-(trifluoromethyl)phenyl)urea (34). ^{1}H NMR (DMSO-d_6) δ 5.23 (s, 2 H), 7.00–7.26 (m, 1 H), 7.39–7.75 (m, 10 H), 9.04 (s, 1 H), 9.21 (s, 1 H). MS (ESI) m/z 413 $(M + H)^+$. Anal. ($C_{21}H_{15}F_3N_4O_2$) C, H, N.

1-(4-(3-Aminobenzo[*d*]isoxazol-4-yl)phenyl)-3-(4-methoxyphenyl)urea (35). ^{1}H NMR (DMSO-d_6) δ 3.72 (s, 3 H), 5.22 (s, 2 H), 6.88 (d, J = 8.82 Hz, 2 H), 7.13 (d, J = 6.44 Hz, 1 H), 7.31–7.53 (m, 5 H), 7.54–7.79 (m, 3 H), 8.54 (s, 1 H), 8.79 (s, 1 H). MS (ESI) m/z 375 $(M + H)^+$. Anal. ($C_{21}H_{18}N_4O_3\cdot 0.15H_2O$) C, H, N.

1-(4-(3-Aminobenzo[*d*]isoxazol-4-yl)phenyl)-3-(4-fluorophenyl)urea (36). ^{1}H NMR (DMSO-d_6) δ 5.22 (s, 2 H), 7.01–7.25 (m, 3 H), 7.35–7.53 (m, 5 H), 7.54–7.73 (m, 3 H), 8.80 (s, 1 H), 8.90 (s, 1 H). MS (ESI) m/z 363 $(M + H^+)$. Anal.($C_{20}H_{15}FN_4O_2$) C, H, N.

1-(4-(3-Aminobenzo[*d*]isoxazol-4-yl)phenyl)-3-(4-(trifluoromethoxy)phenyl)urea (37). ^{1}H NMR (DMSO-d_6) δ 5.22 (s, 2 H), 7.14 (d, J = 7.12 Hz, 1 H), 7.30 (d, J = 9.16 Hz, 2 H), 7.40–7.52 (m, 3 H), 7.54–7.68 (m, 5 H), 8.93 (s, 1 H), 8.96 (s, 1 H). MS (ESI) 429 $(M + H)^+$. Anal. ($C_{21}H_{15}F_3N_4O_3$) C, H, N.

1-(4-(3-Aminobenzo[*d*]isoxazol-4-yl)phenyl)-3-(3,5-dimethylphenyl)urea (38). ^{1}H NMR (DMSO-d_6) δ 2.49 (s, 6 H), 5.47 (s, 2 H), 6.88 (s, 1 H), 7.20–7.46 (m, 3 H), 7.62–7.77 (m, 3 H), 7.78–7.96 (m, 3 H), 8.82 (s, 1 H), 9.08 (s, 1 H). MS (ESI) m/z 373 $(M+ H)^+$. Anal.($C_{22}H_{20}N_4O_2\cdot 0.15H_2O$) C, H, N.

1-(4-(3-Aminobenzo[*d*]isoxazol-4-yl)phenyl)-3-(2-fluoro-5 (trifluoromethyl)phenyl)urea (39). ^{1}H NMR (DMSO-d_6) δ 5.22 (s, 2 H), 7.15 (d, J = 7.12 Hz, 1 H), 7.33–7.70 (m, 8 H), 8.64 (dd, J = 7.29, 2.20 Hz, 1 H), 8.97 (d, J = 2.71 Hz, 1 H), 9.38 (s, 1 H). MS (ESI) m/z 431$(M + H)^+$. Anal. ($C_{21}H_{14}F_4N_4O_2\cdot 0.06CH_2Cl_2$) C, H, N.

1-(4-(3-Aminobenzo[*d*]isoxazol-4-yl)phenyl)-3-(3-fluoro-4-methylphenyl)urea (40). ^{1}H NMR (DMSO-d_6) δ 2.17 (s, 3 H), 5.22 (s, 2 H), 7.05 (dd, J = 8.31, 2.20 Hz, 1 H), 7.10–7.27 (m, 2 H),

7.37–7.53 (m, 4 H), 7.53–7.70 (m, 3 H), 8.84 (s, 1 H), 8.90 (s, 1 H). MS (ESI) *m/z* 377 $(M + H)^+$. Anal. ($C_{21}H_{17}FN_4O_2$) C, H, N.

1-(4-(3-Aminobenzo[*d*]isoxazol-4-yl)phenyl)-3-(4-fluoro-3-(trifluoromethyl)phenyl)urea (41). ^{1}H NMR (DMSO-d_6) δ 5.22 (s, 2 H), 7.14 (d, $J = 7.12$ Hz, 1 H), 7.37–7.52 (m, 4 H), 7.54–7.74 (m, 4 H), 8.03 (dd, $J = 6.44$, 2.71 Hz, 1 H), 9.01 (s, 1 H), 9.11 (s, 1 H). MS (ESI) *m/z* 431 $(M + H)^+$. Anal. ($C_{21}H_{14}F_4N_4O_2$) C, H, N.

1-(4-(3-Aminobenzo[*d*]isoxazol-4-yl)phenyl)-3-(3-chloro-4-fluorophenyl)urea (42). ^{1}H NMR (DMSO-d_6) δ 5.22 (s, 2 H), 7.14 (d, $J = 6.44$ Hz, 1 H), 7.30–7.37 (m, 2 H), 7.41–7.67 (m, 6 H), 7.78–7.86 (m, 1 H), 8.95 (s, 1 H), 8.97 (s, 1 H). MS (ESI) *m/z* 393 $(M + H)^+$. Anal. ($C_{20}H_{14}ClFN_4O_2$) C, H, N.

1-(4-(3-Aminobenzo[*d*]isoxazol-4-yl)phenyl)-3-(3,5-difluorophenyl)urea (43). ^{1}H NMR (DMSO-d_6) δ 5.21 (s, 2 H), 6.71–6.89 (m, 1 H), 7.14 (d, $J = 7.12$ Hz, 1 H), 7.15–7.27 (m, 2 H), 7.39–7.53 (m, 3 H), 7.54–7.70 (m, 3 H), 9.05 (s, 1 H), 9.16 (s, 1 H). MS (ESI) *m/z* 381 $(M + H)^+$. Anal. ($C_{20}H_{14}F_2N_4O_2$) C, H, N.

1-(4-(3-Aminobenzo[*d*]isoxazol-4-yl)phenyl)-3-(3-chloro-4-methoxyphenyl)urea (44). ^{1}H NMR (DMSO-d_6) δ 3.82 (s, 3 H), 5.22 (s, 2 H), 7.02–7.17 (m, 2 H), 7.29 (dd, $J = 8.98$, 2.54 Hz, 1 H), 7.38–7.53 (m, 3 H), 7.53–7.78 (m, 4 H), 8.71 (s, 1 H), 8.87 (s, 1 H). MS (ESI) *m/z* 409 $(M + H)^+$. Anal. ($C_{21}H_{17}ClN_4O_3 \cdot 0.12CH_2Cl_2$) C, H, N.

1-(4-(3-Aminobenzo[*d*]isoxazol-4-yl)phenyl)-3-(3-chloro-4-methylphenyl)urea (45). ^{1}H NMR (DMSO-d_6) δ 2.27 (s, 3 H), 5.22 (s, 2 H), 7.14 (d, $J = 6.10$ Hz, 1 H), 7.17–7.32 (m, 2 H), 7.38–7.54 (m, 3 H), 7.54–7.68 (m, 3 H), 7.71 (d, $J = 2.03$ Hz, 1 H), 8.84 (s, 1 H), 8.91 (s, 1 H). MS (ESI) *m/z* 393 $(M + H)^+$. Anal. ($C_{21}H_{17}ClN_4O_2 \cdot 0.1CH_2Cl_2$) C, H, N.

Compounds **47a**−**e** were prepared using the same procedure described for the synthesis of **7**, substituting compounds **46a**−**e** for compound **6**.

4-Iodo-7-methoxybenzo[*d*]isoxazol-3-amine (47a). ^{1}H NMR (DMSO-d_6) δ 3.91 (s, 3 H), 5.90 (s, 2 H), 6.91 (d, $J = 8.14$ Hz, 1 H), 7.57 (d, $J = 8.14$ Hz, 1 H). MS (ESI) *m/z* 291 $(M + H)^+$.

4-Iodo-7-methylbenzo[*d*]isoxazol-3-amine (47b). ^{1}H NMR (DMSO-d_6) δ 2.36 (s, 3 H), 5.89 (s, 2 H), 7.09 (d, $J = 7.46$ Hz, 1 H), 7.58 (d, $J = 7.46$ Hz, 1 H). MS (ESI) *m/z* 275 $(M + H)^+$.

7-fluoro-4-iodobenzo[*d*]isoxazol-3-amine (47c). ^{1}H NMR (DMSO-d_6) δ 6.09 (s, 2 H), 6.08 (s, 2 H), 7.28 (dd, $J = 10.85$, 8.48 Hz, 1 H), 7.67 (dd, $J = 8.31$, 3.90 Hz, 1 H). MS (ESI) *m/z* 262 $(M + H)^+$.

4-Iodo-7-(morpholinomethyl)benzo[*d*]isoxazol-3-amine (47d). ^{1}H NMR (DMSO-d_6) δ 2.33–2.44 (m, 4 H), 3.52–3.60 (m, 4 H), 3.65 (s, 2 H), 5.92 (s, 2 H), 7.21 (d, $J = 7.46$ Hz, 1 H), 7.67 (d, $J = 7.46$ Hz, 1 H). MS (ESI) *m/z* 360 $(M + H)^+$.

4-Iodo-7-(2-morpholinoethoxy)benzo[*d*]isoxazol-3-amine (47e). ^{1}H NMR (DMSO-d_6) δ 2.37–2.53 (m, 4 H), 2.74 (t, $J = 5.59$ Hz, 2 H), 3.48–3.63 (m, 4 H), 4.25 (t, $J = 5.59$ Hz, 2 H), 5.90 (s, 2 H), 6.94 (d, $J = 8.48$ Hz, 1 H), 7.55 (d, $J = 8.14$ Hz, 1 H). MS (ESI) *m/z* 390 $(M + H)^+$.

4-Bromo-7-(trifluoromethoxy)benzo[*d*]isoxazol-3-amine (47f). To a solution of 6-bromo-2-fluoro-3-(trifluoromethoxy)benzonitrile (2.84 g, 10 mmol) in THF (50 mL) was added *t*-BuOK (1.23 g, 11 mmol). The reaction mixture was stirred for 30 min at room temperature and then acetone oxime (0.80 g, 11mmol) was added. The reaction mixture was stirred for 10 h, then diluted with water, and extracted with ethyl acetate. The organic layer was washed with brine, dried (MgSO4), filtered, and concentrated to dryness. The residue was dissolved in ethanol (20 mL), and 5% HCl (20 mL) was added. The resulting mixture was refluxed for 2 h, and then the solvent was reduced to half-volume. The resulting solid was collected by filtration, and the crude product was purified by flash column chromatography with 0–10% EtOAc in hexane to afford the title compound as a light orange flake (0.95 g, 32%). ^{1}H NMR (DMSO-d_6) δ 6.33 (s, 2 H), 7.46–7.64 (m, 2 H). MS (ESI) *m/z* 299 $(M + H)^+$.

Compounds **48a**−**f** were prepared using the procedure described for the synthesis of **8**, substituting compounds **47a**−**f** for compound **7**.

4-Iodo-7-methoxy-benzo[*d*]isoxazol-3-ylamine (48a). ^{1}H NMR (DMSO-d_6) δ 3.93 (s, 3 H), 5.19 (s, 2 H), 5.31 (s, 2 H), 6.67 (d, $J = 8.48$ Hz, 2 H), 6.94. MS (ESI) *m/z* 256 $(M + H^+)$.

4-(4-Amino-phenyl)-7-methyl-benzo[*d*]isoxazol-3-ylamine (48b). ^{1}H NMR (DMSO-d_6) δ 2.35–2.46 (m, 3 H), 5.19 (s, 1 H), 5.35 (s, 2 H), 6.69 (d, $J = 8.14$ Hz, 2 H), 6.94 (d, $J = 7.46$ Hz, 1 H), 7.13 (d, $J = 8.14$ Hz, 2 H), 7.32 (d, $J = 7.46$ Hz, 1 H). MS (ESI) *m/z* 240 $(M + H^+)$.

4-(4-Aminophenyl)-7-fluorobenzo[*d*]isoxazol-3-amine (48c). ^{1}H NMR (DMSO-d_6) δ 5.36 (s, 2 H), 5.40 (s, 2 H), 6.69 (d, $J = 8.48$ Hz, 2 H), 7.01 (dd, $J = 8.14$, 4.07 Hz, 1 H), 7.14 (d, $J = 8.48$ Hz, 2 H), 7.45 (dd, $J = 10.85$, 8.14 Hz, 1 H). MS (ESI) *m/z* 244 $(M + H^+)$.

4-(4-Aminophenyl)-7-(morpholinomethyl)benzo[*d*]isoxazol-3-amine (48d). ^{1}H NMR (DMSO-d_6) δ 2.30–2.47 (m, 4 H), 3.47–3.64 (m, 4 H), 3.70 (s, 2 H), 5.21 (s, 2 H), 5.38 (s, 2 H), 6.69 (d, $J = 8.48$ Hz, 2 H), 7.02 (d, $J = 7.46$ Hz, 1 H), 7.15 (d, $J = 8.48$ Hz, 2 H), 7.45 (d, $J = 7.46$ Hz, 1 H). MS (ESI) *m/z* 325 $(M + H)^+$.

4-(4-Aminophenyl)-7-(2-morpholinoethoxy)benzo[*d*]isoxazol-3-amine (48e). ^{1}H NMR (DMSO-d_6) δ 2.40–2.56 (m, 4 H), 2.76 (t, $J = 5.59$ Hz, 2 H), 3.52–3.63 (m, 4 H), 4.28 (t, $J = 5.59$ Hz, 2 H), 5.19 (s, 2 H), 5.31 (s, 2 H), 6.58–6.75 (m, 2 H), 6.92 (d, $J = 7.80$ Hz, 1 H), 7.04–7.16 (m, 3 H). MS (ESI) *m/z* 355 $(M + H)^+$.

4-(4-Aminophenyl)-7-(trifluoromethoxy)benzo[*d*]isoxazol-3-amine (48f). ^{1}H NMR (DMSO-d_6) δ 5.42 (s, 2 H), 5.46 (s, 2 H), 6.70 (d, $J = 8.48$ Hz, 2 H), 7.11 (d, $J = 8.14$ Hz, 1 H), 7.14–7.23 (m, 2 H), 7.60 (dd, $J = 8.14$, 1.36 Hz, 1 H). MS (ESI) *m/z* 310 $(M + H^+)$.

Compounds **49**–**57** were prepared using the procedure described for the synthesis of **13** (method B) substituting compounds **48a**−**f** for compound **8**.

1-(4-(3-Amino-7-methoxybenzo[*d*]isoxazol-4-yl)phenyl)-3-(2-fluoro-5 methylphenyl)urea (49). ^{1}H NMR (DMSO-d_6) δ 2.28 (s, 3 H), 3.96 (s, 3 H), 5.21 (s, 2 H), 6.75–6.87 (m, 1 H), 7.00–7.21 (m, 3 H), 7.30–7.45 (m, 2 H), 7.52–7.69 (m, 2 H), 8.00 (dd, $J = 7.63$, 1.86 Hz, 1 H), 8.53 (d, $J = 2.71$ Hz, 1 H), 9.22 (s, 1 H). MS (ESI) *m/z* 407 $(M + H)^+$. Anal. ($C_{22}H_{19}FN_4O_3$) C, H, N.

1-(4-(3-Amino-7-methoxybenzo[*d*]isoxazol-4-yl)phenyl)-3-(3(trifluoromethyl)phenyl)urea (50). ^{1}H NMR (DMSO-d_6) δ 3.96 (s, 3 H), 5.21 (s, 2 H), 7.05 (d, $J = 7.80$ Hz, 1 H), 7.17 (d, $J = 8.14$ Hz, 1 H), 7.32 (d, $J = 7.46$ Hz, 1 H), 7.39 (d, $J = 8.48$ Hz, 2 H), 7.53 (t, $J = 7.80$ Hz, 1 H), 7.61 (m, 3 H), 8.04 (s, 1 H), 8.96 (s, 1 H), 9.10 (s, 1 H). MS (ESI) *m/z* 443 $(M + H)^+$. Anal. ($C_{22}H_{17}F_3N_4O_3 \cdot 0.15CH_2Cl_2$) C, H, N.

1-(4-(3-Amino-7-methoxybenzo[*d*]isoxazol-4-yl)phenyl)-3-(3-chlorophenyl)urea (51). ^{1}H NMR (DMSO-d_6) δ 3.96 (s, 3 H), 5.20 (s, 2 H), 7.00–7.06 (m, 2 H), 7.16 (d, $J = 8.14$ Hz, 1 H), 7.25–7.35 (m, 2 H), 7.39 (d, $J = 8.81$ Hz, 2 H), 7.60 (d, $J = 8.48$ Hz, 2 H), 7.73 (t, $J = 2.03$ Hz, 1 H), 8.92 (s, 1 H), 8.94 (s, 1 H). MS (ESI) *m/z* 409 $(M + H)^+$. Anal. ($C_{21}H_{17}ClN_4O_3$) C, H, N.

1-(4-(3-Amino-7-methoxybenzo[*d*]isoxazol-4-yl)phenyl)-3-(3-bromophenyl)urea (52). ^{1}H NMR (DMSO-d_6) δ 3.96 (s, 3 H), 5.21 (s, 2 H), 6.96–7.09 (m, 1 H), 7.12–7.47 (m, 6 H), 7.60 (d, $J = 8.48$ Hz, 2 H), 7.88 (t, $J = 2.03$ Hz, 1 H), 8.92 (d, $J = 3.05$ Hz, 2 H). MS (ESI) *m/z* 453 $(M + H)^+$. Anal. ($C_{21}H_{17}BrN_4O_3$) C, H, N.

1-(4-(3-Amino-7-methylbenzo[*d*]isoxazol-4-yl)phenyl)-3-(2-fluoro-5-methylphenyl)urea (53). ^{1}H NMR (DMSO-d_6) δ 2.28 (s, 3 H), 2.45 (s, 3 H), 5.20 (s, 2 H), 6.71–6.90 (m, 1 H), 6.96–7.20 (m, 2 H), 7.31–7.49 (m, 3 H), 7.51–7.74 (m, 2 H), 8.00 (dd, $J = 7.63$, 1.86 Hz, 1 H), 8.54 (d, $J = 2.37$ Hz, 1 H); 9.24 (s, 1 H). MS (ESI) *m/z* 391 $(M + H)^+$. Anal. ($C_{22}H_{19}FN_4O_2 \cdot 0.1H_2O$) C, H, N.

1-(4-(3-Amino-7-fluorobenzo[*d*]isoxazol-4-yl)phenyl)-3-(2-fluoro-5-methylphenyl)urea (54). ^{1}H NMR (DMSO-d_6) δ 2.28 (s, 3 H), 5.38 (s, 2 H), 6.73–6.89 (m, 1 H), 7.05–7.19 (m, 2 H), 7.39–7.46 (m, 2 H), 7.52 (dd, $J = 10.85$, 8.14 Hz, 1 H), 7.62 (d, $J = 8.81$ Hz, 2 H), 8.00 (dd, $J = 7.63$, 1.86 Hz, 1 H), 8.55 (d, $J = 2.37$ Hz, 1 H), 9.25 (s, 1 H). MS (ESI) *m/z* 395 $(M + H)^+$. Anal. ($C_{21}H_{16}F_2N_4O_2 \cdot 0.1$hexane$\cdot 0.2H_2O$) C, H, N.

1-(4-(3-Amino-7-(trifluoromethoxy)benzo[*d*]isoxazol-4-yl)phenyl)-3-(2-fluoro-5-methylphenyl)urea (55). ^{1}H NMR (DMSO-d_6) δ 2.28 (s, 3 H), 5.44 (s, 2 H), 6.75–6.92 (m, 1 H), 7.05–7.26 (m, 2 H), 7.47 (d, J = 8.82 Hz, 2 H), 7.56–7.78 (m, 3 H), 8.00 (dd, J = 7.97, 1.86 Hz, 1 H), 8.56 (d, J = 2.71 Hz, 1 H), 9.28 (s, 1 H). MS (ESI) m/z 461 $(M + H)^+$. Anal. ($C_{22}H_{16}F_4N_4O_3$) C, H, N.

1-(4-(3-Amino-7-(morpholinomethyl)benzo[*d*]isoxazol-4-yl)phenyl)-3-(2-fluoro-methylphenyl)urea (56). ^{1}H NMR (DMSO-d_6) δ 2.28 (s, 3 H), 2.35–2.48 (m, 4 H), 3.50–3.65 (m, 4 H), 3.74 (s, 2 H), 5.23 (s, 2 H), 6.75–6.85 (m, J = 2.37 Hz, 1 H), 7.05–7.18 (m, 2 H), 7.44 (d, J = 8.48 Hz, 2 H), 7.52 (d, J = 7.80 Hz, 1 H), 7.62 (d, J = 8.48 Hz, 2 H), 8.00 (dd, J = 7.80, 1.70 Hz, 1 H), 8.55 (d, J = 2.37 Hz, 1 H), 9.25 (s, 1 H). MS (ESI) m/z 476 $(M + H)^+$. Anal. ($C_{26}H_{26}FN_5O_3 \cdot 0.1CH_2Cl_2$) C, H, N.

1-(4-(3-Amino-7-(2-morpholinoethoxy)benzo[*d*]isoxazol-4-yl)phenyl)-3-(2-fluoro-5-methylphenyl)urea (57). ^{1}H NMR (DMSO-d_6) δ 2.28 (s, 3 H), 2.45–2.55 (m, 4 H), 2.78 (t, J = 5.59 Hz, 2 H), 3.50–3.65 (m, 4 H), 4.31 (t, J = 5.76 Hz, 2 H), 5.21 (s, 2 H), 6.75–6.84 (m, 1 H), 7.03 (d, J = 8.14 Hz, 1 H), 7.11 (dd, J = 11.36, 8.31 Hz, 1 H), 7.19 (d, J = 8.14 Hz, 1 H), 7.39 (d, J = 8.48 Hz, 2 H), 7.59 (d, J = 8.48 Hz, 2 H), 8.00 (dd, J = 7.80, 2.03 Hz, 1 H), 8.53 (d, J = 2.37 Hz, 1 H), 9.22 (s, 1 H). MS (ESI) m/z 506 $(M + 1)^+$. Anal. ($C_{27}H_{28}FN_5O_4$) C, H, N.

References

(1) Hubbard, S. R.; Till, J. H. Protein Tyrosine Kinases Structure and Function. *Annu. Rev. Biochem.* **2000**, *69*, 373–398.

(2) Ullrich, A.; Schlessinger, J. Signal Transduction by Receptors with Tyrosine Kinase Activity. *Cell* **1990**, *61*, 203–212.

(3) Strawn, L. M.; Shawver, L. K. Tyrosine Kinases in Disease: Overview of Kinase Inhibitors as Therapeutic Agents and Current Drugs in Clinical Trials. *Expert Opin. Invest. Drugs* **1998**, *7*, 553–573.

(4) Bardelli, A.; Parsons, D. W.; Silliman, N.; Ptak, J.; Szabo, S.; Saha, S.; Markowitz, S.; Willson, J. K. V.; Parmigiani, G.; Kinzler, K. W.; Vogelstein, B.; Velculescu, V. E. Mutational Analysis of the Tyrosine Kinome in Colorectal Cancers. *Science* **2003**, *300*, 949–949.

(5) Blume-Jensen, P.; Hunter, T. Oncogenic Kinase Signaling. *Nature* **2001**, *411*, 355–365.

(6) Ferrara, N.; Gerber, H.-P.; LeCouter, J. The Biology of VEGF and Its Receptor. *Nat. Med.* **2003**, *9*, 669–676.

(7) Shalaby, F.; Rossant, J.; Yamaguchi, T. P.; Gertsenstein, M.; Wu, X.-F.; Breitman, M. L.; Schuh, A. C. Failure of Blood-island Formation and Vasculogenesis in Flk-1-deficient Mice. *Nature* **1995**, *376*, 62–65.

(8) Bilodeau, M. T.; Fraley, M. E.; Hartman, G. D. Kinases Insert Domain-Containing Receptor Kinase Inhibitors as Antiangiogenic Agents. *Expert Opin. Invest. Drugs* **2002**, *11*, 737–745.

(9) Kim, I.; Kim, H. G.; Moon, S.-O.; Chae, S. W.; So, J.-N.; Koh, K. N.; Ahn, B. C.; Koh, G. Y. Angiopoietin-1 Induces Endothelial Cell Sprouting Through the Activation of Focal Adhesion Kinase and Plasmin Secretion. *Circ. Res.* **2000**, *86*, 952–959.

(10) Yancopoulos, G. D.; Davis, S.; Gale, N. W.; Rudge, J. S.; Wiegand, S. J.; Holash, J. Vascular-Specific Growth Factors and Blood Vessel Formation. *Nature* **2000**, *407*, 242–248.

(11) Wang, D.; Huang, H.-J. S.; Kazlauskas, A.; Cavenee, W. K. Induction of Vascular Endothelial Growth Factor Expression in Endothelial Cells by Platelet-Derived Growth Factor Through the Activation of Phosphatidylinositol 3-Kinase. *Cancer Res.* **1999**, *59*, 1464–1472.

(12) Lindahl, P.; Johansson, B. R.; Levéen, P.; Betsholtz, C. Pericyte Loss and Microaneurysm Formation in PDGF-B-Deficient Mice. *Science* **1997**, *277*, 242–245.

(13) Demetri, G. D. Targeting c-Kit Mutations in Solid Tumors: Scientific Rationale and Novel Therapeutic Options. *Semin. Oncol.* **2001**, *28*, 19–26.

(14) Armstrong, S. A.; Kung, A. L.; Mabon, M. E.; Silverman, L. B.; Stam, R. W.; Den Boer, M. L.; Pieters, R.; Kersey, J. H.; Sallan, S. E.; Fletcher, J. A.; Golub, T. R.; Griffin, J. D.; Korsmeyer, S. J. Inhibition of FLT3 in MLL: Validation of a Therapeutic Target Identified by Gene Expression Based on Classification. *Cancer Cell* **2003**, *3*, 173–183.

(15) Sawyers, C. L. Finding the Next Gleevec: FLT3 Targeted Kinase Inhibitor Therapy for Acute Myeloid Leukemia. *Cancer Cell* **2002**, *1*, 413–415.

(16) Lux, M. L.; Rubin, B. P.; Biase, T. L.; Chen, C.-J.; Maclure, T.; Demetri, G.; Xiao, S.; Singer, S.; Fletcher, C. D. M.; Fletcher, J. A. KIT Extracellular and Kinase Domain Mutations in Gastrointestinal Stromal Tumors. *Am. J. Pathol.* **2002**, *156*, 791–5.

(17) Stirewalt, D. L.; Radich, J. P. The Role of FLT3 in Haematopoietic Malignancies. *Nat. Rev. Cancer* **2003**, *3*, 650–665.

(18) Banerji, L.; Sattler, M. Targeting Mutated Tyrosine Kinases in the Therapy of Myeloid Leukemias. *Expert Opin. Ther. Targets* **2004**, *8*, 221–239.

(19) Eskens, F. Angiogenesis Inhibitors in Clinical Development; Where Are We Now and Where Are We Going. *Br. J. Cancer* **2004**, *90*, 1–7.

(20) Gschwind, A.; Fisher, O. M.; Ullrich, A. The Discovery of Receptor Tyrosine Kinases: Targets for Cancer Therapy. *Nat. Rev. Cancer* **2004**, *4*, 361–370.

(21) Vieth, M.; Sutherland, J. J.; Robertson, D. H.; Campbell, R. M. Kinomics: Characterizing the Therapeutically Validated Kinase Space. *Drug Discovery Today* **2005**, *10*, 839–846.

(22) Fox, W. D.; Higgins, B.; Maiese, K. M.; Drobnjak, M.; Cordon-Cardo, C.; Scher, H. I.; Agus, D. B. Antibody to Vascular Endothelial Growth Factor Slows Growth of Androgen-independent Xenograft Model of Prostate Cancer. *Clin. Cancer Res.* **2001**, *8*, 3226–3231.

(23) Stopeck, A.; Sheldon, M.; Vahedian, M.; Cropp, G.; Gosalia, R.; Hannah, A. Results of a Phase I Dode-Escalating Study of the Antiangiogenic Agent, SU5416, in Patients with Advanced Malignancies. *Clin. Cancer Res.* **2002**, *8*, 2798–2805.

(24) Bold, G.; Altmann, K.-H.; Frei, J.; Lang, M.; Manley, P. W.; Traxler, P.; Wietfeld, B.; Brüggen, J.; Buchdunger, E.; Cozens, R.; Ferrari, S.; Furet, P.; Hofmann, F.; Martiny-Baron, G.; Mestan, J.; Rösel, J.; Sills, M.; Stover, D.; Acemoglu, F.; Boss, E.; Emmenegger, R.; Lässer, L.; Masso, E.; Roth, R.; Schlachter, C.; Vetterli, W.; Wyss, D.; Wood, J. M. New Anilinophthalazines as Potent and Orally Well Absorbed Inhibitors of the VEGF Receptor Tyrosine Kinases Useful as Antagonists of Tumor-Driven Angiogenesis. *J. Med. Chem.* **2000**, *43*, 2310–2323.

(25) Wood, J. M.; Bold, G.; Buchdunger, E.; Cozens, R.; Ferrari, S.; Frei, J.; Hofmann, F.; Mestan, J.; Mett, H.; O'Reilly, T.; Persohn, E.; Rösel, J.; Schnell, C.; Stover, D.; Theuer, A.; Towbin, H.; Wenger, F.; Woods-Cook, K.; Menrad, A.; Siemeister, G.; Schirner, M.; Thierauch, K.-H.; Schneider, M. R.; Drevs, J.; Martiny-Baron, G.; Totzke, F.; Marmé, D. PTK787/ZK222584, A Novel and Potent Inhibitor of Vascular Endothelial Growth Factor Receptor Tyrosine Kinases, Impairs Vascular Endothelial Growth Factor-induced Responses and Tumor Growth after Oral Administration. *Cancer Res.* **2000**, *60*, 2178–2189.

(26) Roberts, W. G.; Jani, J.; Beebe, J.; Emerson, E.; Gant, T.; Goodwin, P.; Higdon, C.; Hillerman, S.; Intrieri, C.; Knauth, E.; Marx, M.; Noe, M.; Rossi, A. M.; Savage, D.; Atherton, J.; Schaeffer, T.; Floyd, E.; Harriman, S. Preclincal Development of CP-547,632, a Novel VEGFR-2 Inhibitor for Cancer Therapy. Proceedings of the American Society of Clinical Oncology, 2002, Abstract #473.

(27) Yoshiji, H.; Harris, S. R.; Thorgeirsson, U. P. Vascular Endothelial Growth Factor Is Essential for Initial But Not Continued In Vivo Growth of Human Breast Carcinoma Cells. *Cancer Res.* **1997**, *57*, 3924–3928.

(28) Bergers, G.; Javaherian, K.; Lo, K. M.; Folkman, J.; Hanahan, D. Effects of Angiogenesis Inhibitors on Multistage Carcinogenesis in Mice. *Science* **1999**, *284*, 808–812.

(29) Carmeliet, P. Angiogenesis in Health and Disease. *Nat. Med.* **2003**, *9*, 653–660.

(30) Mandel, D. B.; Laird, A. D.; Xin, X.; Louie, S. G.; Christensen, J. G.; Li, G.; Schreck, R. E.; Abrams, T. J.; Ngai, T. J.; Lee, L. B.; Murray, L. J.; Carver, J.; Chan, E.; Moss, K. G.; Haznedar, J. O.; Sukbuntherng, J.; Blake, R. A.; Sun, L.; Tang, C.; Miller, T.; Shirazian, S.; McMahon, G.; Cherrington, J. M. In Vivo Antitumor Activity of SU11248, A Novel Tyrosine Kinase Inhibitor Targeting Vascular Endothelial Growth Factor and Platelet-derived Growth Factor Receptors: Determination of a Phamarcokinetic/Pharmacodynamic Relationship. *Clin. Cancer Res.* **2003**, *9*, 327–337.

(31) Wilhelm, S. M.; Carter, C.; Tang, L.; Wilkie, D.; McNabola, A.; Rong, H.; Chen, C.; Zhang, X.; Vincent, P.; McHugh, M.; Cao, Y.; Shujath, J.; Gawlak, S.; Eveleigh, D.; Rowley, B.; Liu, L.; Adnane, L.; Lynch, M.; Auclair, D.; Taylor, I.; Gedrich, R.; Voznesensky, A.; Riedl, B.; Post, L. E.; Bollag, G.; Trail, P. A. BAY 43–9006 Exhibits Broad Spectrum Oral Antitumor Activity and Targets the RAF/MEK/ERK Pathway and Receptor Tyrosine Kinases Involved in Tumor Progression and Angiogenesis. *Cancer Res.* **2004**, *64*, 7099–7109.

(32) Dai, Y.; Guo, Y.; Frey, R. R.; Ji, Z.; Curtin, M. L.; Ahmed, A. A.; Albert, D. H.; Arnold, L.; Arries, S. S.; Barlozzari, T.; Bauch, J. L.; Bouska, J. J.; Bousquet, P. F.; Cunha, G. A.; Glaser, K. B.; Guo, J.; Li, J.; Marcotte, P. A.; Marsh, K. C.; Moskey, M. D.; Pease, L. J.; Stewart, K. D.; Stoll, V. S.; Tapang, P.; Wishart, N.; Davidsen, S. K.; Michaelides, M. R. Thienopyrimidine Ureas as Novel Potent Multitargeted Receptor Tyrosine Kinases Inhibitors. *J. Med. Chem.* **2005**, *48*, 6066–6083.

(33) Ji, Z.; Ahmed, A. A.; Albert, D. H.; Bouska, J. J.; Bousquet, P. F.; Cunha, G. A.; Glaser, K. B.; Guo, J.; Li, J.; Marcotte, P. A.;

Moskey, M.; D.; Pease, L. J.; Stewart, K. D.; Yates, M.; Davidsen, S. K.; Michaelides, M. R. Isothiazolopyrimidines and Isoxazolopyrimidines as Novel Multi-Targeted Inhibitors of Receptor Tyrosine Kinases. *Bioorg. Med. Chem. Lett.* **2006**, *16*, 4326–4330.

(34) Heyman, H. R.; Frey, R. R.; Bousquet, P. F.; Cunha, G. A.; Moskey, M. D.; Ahmed, A. A.; Soni, N. B.; Marcotte, P. A.; Pease, L. J.; Glaser, K. B.; Yates, M.; Bouska, J. J.; Albert, D. H.; Black-Schaefer, C. L.; Dandliker, P. J.; Stewart, K. D.; Rafferty, P.; Davidsen, S. K.; Michaelides, M. R.; Curtin, M. L. *Bioorg. Med. Chem. Lett.* **2007**, *17*, 1246–1249.

(35) Dai, Y.; Hartandi, K.; Ji, Z.; Ahmed, A. A.; Albert, D. H.; Bauch, J. L.; Bouska, J. J.; Bousquet, P. F.; Cunha, G. A.; Glaser, K. B.; Harris, C. M.; Hickman, D.; Guo, J.; Li, J.; Marcotte, P. A.; Marsh, K. C.; Moskey, M. D.; Martin, R. L.; Olson, A. M.; Osterling, D. J.; Pease, L. J.; Soni, N. B.; Stewart, K. D.; Stoll, V. S.; Tapang, P.; Reuter, D. R.; Davidsen, S. K.; Michaelides, M. R. Discovery of *N*-(4-(3-Amino-1*H*-indazol-4-yl)phenyl)-*N*′-(2-fluoro-5-methylphenyl)urea (ABT-869), a 3-Aminoindazole-Based Orally Active Multitargeted Receptor Tyrosine Kinase Inhibitor. *J. Med. Chem.* **2007**, *50*, 1584–1597.

(36) Albert, D. H.; Tapang, P.; Magoc, T. J.; Pease, L. J.; Reuter, D. R.; Wei, R.-Q.; Li, J.; Guo, J.; Bousquet, P. F.; Ghoreishi-Haack, N. S.; Wang, B.; Bukofzer, G. T.; Wang, Y.-C.; Stavropoulos, J. A.; Hartandi, K.; Niquette, A. L.; Soni, N.; Johnson, E. F.; McCall, J. O.; Bouska, J. J.; Luo, Y.; Donawho, C. K.; Dai, Y.; Marcotte, P. A.; Glaser, K. B.; Michaelides, M. R.; Davidsen, S. K. Preclinical Activity of ABT-869, A Multitargeted Receptor Tyrosine Kinase Inhibitor. *Mol. Cancer Ther.* **2006**, *5*, 995–1006.

(37) The plasma exposure ($AUC_{0-24\ h}$) at the last day of study for **50** (10mg/kg/day) was 13.2 μM·hr; in comparison, **3** displayed similarly robust 85% inhibition at a 30 mg/kg/day bid dose, resulting in terminal plasma exposure ($AUC_{0-24\ h}$) of 19.1 μM·hr.

JM701096V